Korean J. Chem. Eng., **15**(6), 637-643 (1998)

REMOVAL AND RECOVERY OF HEAVY METAL IONS IN FIXED AND SEMI-FLUIDIZED BEDS

Seung Jai Kim†, Suk Young Jeung and Hee Moon*

Department of Environmental Engineering, *Faculty of Applied Chemical Engineering,
Chonnam National University, Kwangju 500-757, Korea
(Received 28 March 1998 • accepted 15 June 1998)

Abstract – Uptakes of heavy metal ions such as Pb^{2+} and Ni^{2+} were studied experimentally in fixed and semi-fluidized beds packed with a strong cation exchange resin, Amberlite 200. Single and binary aqueous solutions of lead and nickel ions were passed through ion exchange columns, and the exit concentrations were measured to get the breakthrough behavior of the ions. From the exit concentration profiles, the breakthrough time and the ion exchange capacity were evaluated. After removal of heavy metal ions from binary solution of lead and nickel ions until the breakthrough time, two metal ions were recovered by precipitation and resolubilization of lead. In this paper, the recovery yield and separation efficiency are rigorously discussed.

Key words: Removal and Recovery, Ion-Exchange, Fixed Bed, Semi-Fluidized Bed, Lead, Nickel

INTRODUCTION

Wastewater containing heavy metal ions such as lead, nickel, cadmium, and copper is generated by circuit board industries [Haas and Tare, 1984]. Environmental concerns make it is necessary to remove heavy metal ions from the wastewater. In addition, the recovery of heavy metal ions is also required to reuse them. The most common method of eliminating heavy metal ions from wastewater is precipitation [Patterson, 1975], but metal ions cannot be removed by precipitation below the level of its solubility [Maruyama et al., 1975]. Furthermore, precipitation has a series of accompanying problems such as sludge increase by chemical addition, sludge treatment, and separation of heavy metal ions from sludge. Therefore the ion-exchange process using fixed, semi-fluidized, and fluidized beds would be applied as a promising method to remove or separate heavy metal ions from wastewater [Fan et al., 1959, 1960].

The design of such a separator requires basic information for the flow and liquid-solid mass transfer [Anderson, 1988; Singh et al., 1980]. In this work mass transfer between liquid and ion exchange resin particles was studied experimentally in fixed and semi-fluidized beds of a strong cation exchanger, Amberlite 200. Single and binary aqueous solutions of nickel and lead ions were passed through the column packed with ion exchange particles to get their breakthrough curves. These experiments enabled us to evaluate the breakthrough time and the ion exchange capacity for two metal ions.

After simultaneous removal of lead and nickel ions from binary solutions until the predetermined breakthrough time, additional experiments were carried out to recover heavy metal ions separately by precipitation and resolubilization of lead in the same bed. This recovery process consists of three major steps: removal of heavy metal ions until the breakthrough time, precipitation of lead as $PbCl_2$, and resolubilization of precipitate [Lee and Hong, 1995]. Furthermore the recovery yield and the separation efficiency were also studied with and without the precipitation step.

†To whom all correspondence should be addressed.
E-mail: sjkim@chonnam.chonnam.ac.kr

EXPERIMENTS

An ion-exchange column was made of an acrylic tube of 40 mm diameter and 380 mm length. The pressures along the column were measured using pressure taps attached on the column wall. The lower part of the column of 150 mm height was packed with beads to distribute the solution uniformly. A movable particle-retaining grid, which is made of a 100-mesh stainless steel net, was also fixed in the column to use it as a fixed bed or a semi-fluidized bed according to its purpose.

The exit concentrations of nickel and lead ions were analyzed by ICP (Model: TY 38 plus, Jobin Yvon Company). A strong cation exchange resin of sodium form, Amberlite 200 (Rohm and Haas Co.), was used as a separating medium. The resin particles in the swollen state were sieved with a set of standard sieves to get uniform particles. The average particle size was 0.57 mm (20/50 mesh). The water content of the resin was determined by drying resin particles in an oven at 110 °C for 24 hours. The water content was about 43 %. Distilled water was used to make single and binary working solutions of nickel and lead. The temperature of solutions was kept at 30 ± 2 °C during experiments.

In each experiment, a known amount of resin particles were loaded into the column and distilled water was passed through it to measure the minimum fluidization velocity, pressure drop, and bed expansion. Also the heights of the upper packed bed and lower fluidized bed sections in a semi-fluidized state were measured. Experiments in the semi-fluidized bed were repeated by varying the position of the retaining grid and the fluid

velocity.

The separation factor between Pb^{2+} and Ni^{2+} on the resin was determined by measuring the concentrations of two ions remaining in the vessel after equilibrium was reached. The vessel was shaken in a thermostat at 25 °C for three days. In this experiment, about 2.5 g of resin particles was contacted with solutions. The ion exchange equilibrium isotherms of two metal ions on the resin were determined from the experimental data above.

Single and binary breakthrough curves in fixed and semi-fluidized beds were obtained experimentally as follows. Solutions of Ni^{2+} and Pb^{2+} were passed through the column that was packed with about 50 g of the ion exchange resin in dry state and the exit concentrations were monitored until the column was fully saturated.

RESULTS AND DISCUSSION

1. Bed Height and Pressure Drop

In this study, U_{mf} of resin particles with 0.57 mm mean diameter measured experimentally in the fluidized bed was 1.33 mm/s. U_t was calculated theoretically as 35.8 mm/s [Davidson and Harrison, 1997]. The heights of both the fluidized bed and packed bed sections in the semi-fluidized bed were measured. The initial height of the loosely packed bed (h_0) was 64 mm, and the heights of the retaining grid (h) were 76, 85, and 100 mm. As shown in Fig. 1, the height of the fluidized bed section decreases as the fluid velocity is increased, while that for the packed bed section increases for U < 15 mm/s. The increase in heights is small above this velocity.

The pressure drop in a semi-fluidized bed is shown in Fig. 2. In a fixed bed, the pressure drop increases practically linearly with the fluid velocity. In a fluidized bed, the pressure drop increases with the fluid velocity for $U < U_{mf}$, but it is practically constant above U_{mf}. The pressure profile in a semi-fluidized bed could be explained by dividing the bed into two sections, the packed bed section and the fluidized bed section. As the fluid velocity increases above U_{mf}, the bed expands and the particles in the beds are fluidized. When the fluid velocity increases above a certain value, 5 mm/s, the bed expansion is restricted by the particle retaining grid and the bed is separated into two sections: the lower fluidized-bed section and the upper packed-bed section. As shown in Fig. 2, the pressure drop in the upper packed bed section is dominant, especially as the fluid velocity is increased and the retaining grid height is decreased.

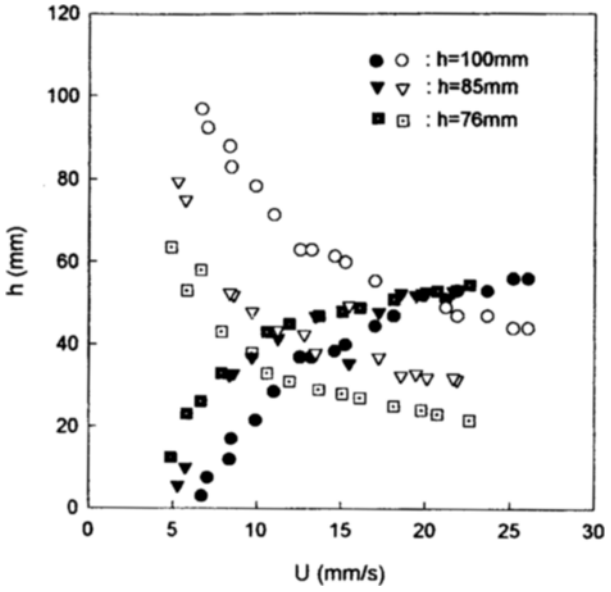

Fig. 1. Height of the packed bed section and fluidized bed section in semi-fluidized beds for different retaining grid heights.
d_p=0.57 mm, h_o=64 mm, resin weight=50 g, ●▼■: packed bed section, ○▽⊡: fluidized bed section

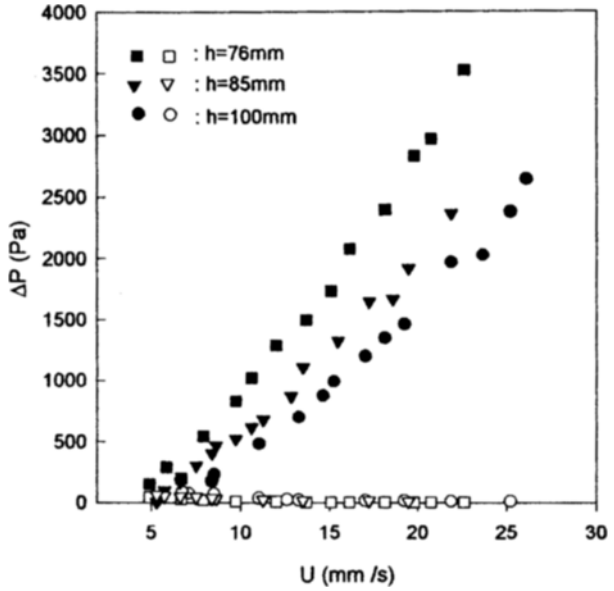

Fig. 2. Pressure drop in the semi-fluidized beds for different retaining grid heights.
h_o=64 mm, h=76, 85, 100 mm, resin weight=50 g, ●▼■: packed bed section ○▽□: fluidized bed section

Considering the variations of the packed bed section height and the pressure drop in that section with liquid velocity, the pressure drop increase due to the fluid-particle drag is dominant for U > 15 mm/s.

2. Equilibrium Isotherm

Among well-known isotherm equations, the Langmuir equation was applied to fit ion exchange equilibrium data of Ni^{2+} or Pb^{2+} on Amberlite 200 at 25 °C as follows:

$$Q = \frac{25.100Ce}{1+0.062Ce} \quad \text{for lead} \tag{1}$$

$$Q = \frac{2.709Ce}{1+0.021Ce} \quad \text{for nickel} \tag{2}$$

where Ce and Q are the equilibrium ion concentration in the liquid phase (mg/*l*) and the ion-exchange capacity per unit mass of resin (mg/g resin), respectively. As shown in Fig. 3, the ion-exchange equilibrium data of Pb^{2+} or Ni^{2+} on Amberlite 200 can be fitted with the Langmuir equation.

The separation factors, α_{ij}, between two metal ions for the resin were determined from binary ion-exchange equilibrium data as shown in Fig. 4. According to Clifford [1976], the sep-

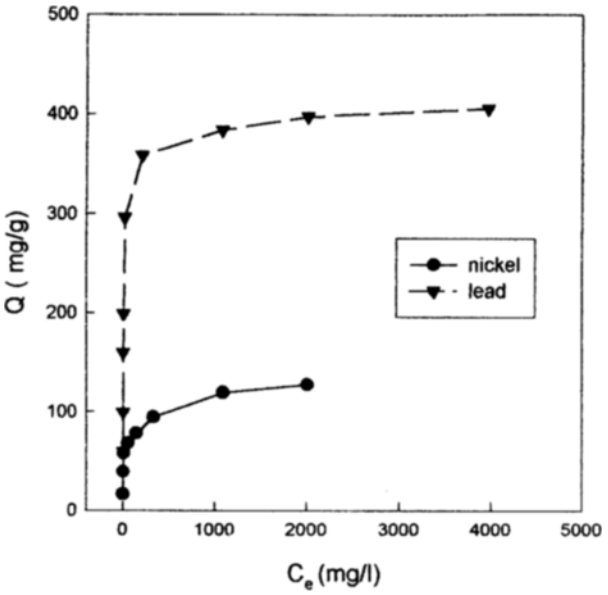

Fig. 3. Ion exchange isotherms of Pb^{+2} and Ni^{+2} ions (at 25 °C).

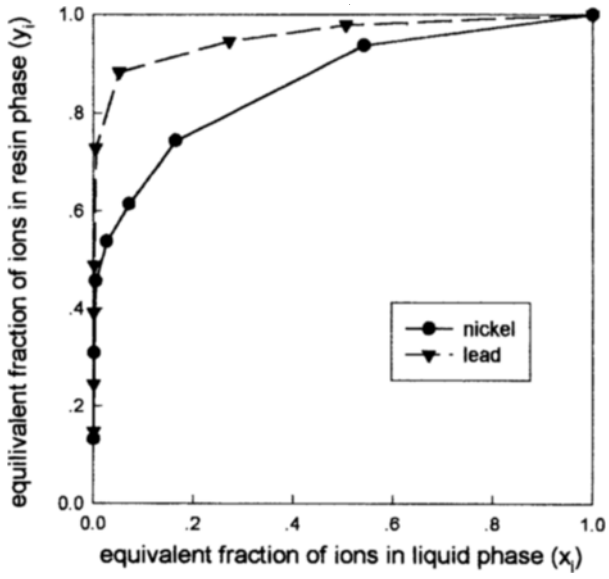

Fig. 4. Binary ion exchange isotherms of Pb^{2+}/Na^{+} and Ni^{+2}/Na^{+} (at 25 °C).

aration factor could be determined from the following equation.

$$R = \frac{\text{area below isotherm}}{\text{area above isotherm}} = \frac{(\alpha^2 - \alpha - \alpha \ln \alpha)/(\alpha - 1)^2}{1 - [(\alpha^2 - \alpha - \alpha \ln \alpha)/(\alpha - 1)^2]} \quad (3)$$

Once the areas above and below the binary isotherm shown in Fig. 4 are known, Eq. (3) can be solved by a trial and error method to give the value of the separation factor for a given binary system. To evaluate the areas precisely requires accurate isotherm data. Detailed calculation procedures are given elsewhere [Clifford, 1976]. The separation factors calculated from Eq. (3) are $\alpha_{Pb/Na}$=75.9, $\alpha_{Ni/Na}$=14.1, respectively. Therefore the selectivity for Pb^{2+} on Amberlite 200 is much larger than that for Ni^{2+}.

3. Breakthrough Curves for Single Component Solution

Figs. 5 and 6 show the single-component breakthrough curves of Pb^{2+} and Ni^{2+} in a fixed, semi-fluidized, and fluidized bed, respectively. From experimental breakthrough curves, it is shown that the fixed bed operation gives the most stiff curve. This result is quite natural since the axial dispersion coefficient in the fixed bed operation is smaller than other cases. In this work, the breakthrough time was defined as the time at which the exit concentration reaches 10 % of the inlet concentration. The breakthrough curves of Pb^{2+} and Ni^{2+} in the semi-fluidized bed lie between those of the fixed and fluidized beds [Hwang and Lu, 1995]. This result could be expected from the fact that the semi-fluidized bed possesses the features of both fixed and fluidized beds. Two figures also show that the exit concentration from the fluidized bed is higher than

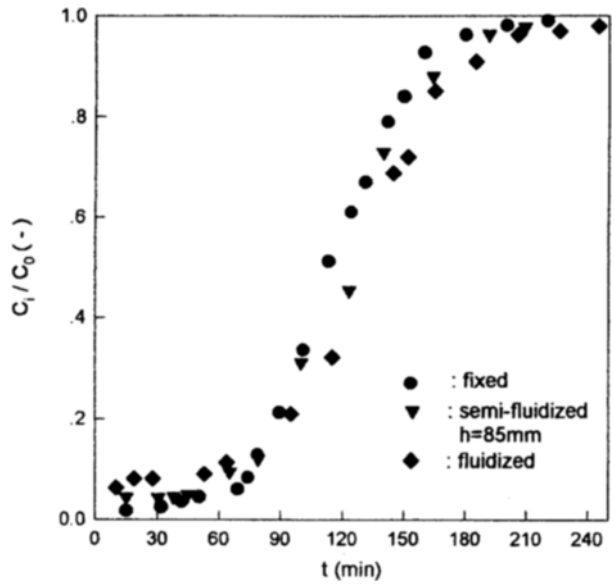

Fig. 5. Breakthrough data of Ni^{+2} ions in the fixed bed, fluidized bed and semi-fluidized bed.
C_{Ni}= 3 mN, U=5.33 U_{mf}, resin weight=50 g

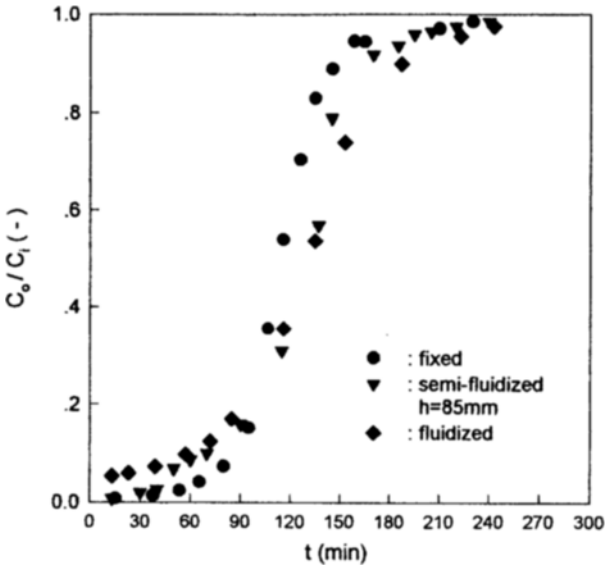

Fig. 6. Breakthrough curves of Pb^{+2} ions in the fixed bed, fluidized bed, semi-fluidized bed.
C_{Pb}= 3 mN, U=5.33 U_{mf}, resin weight=50 g

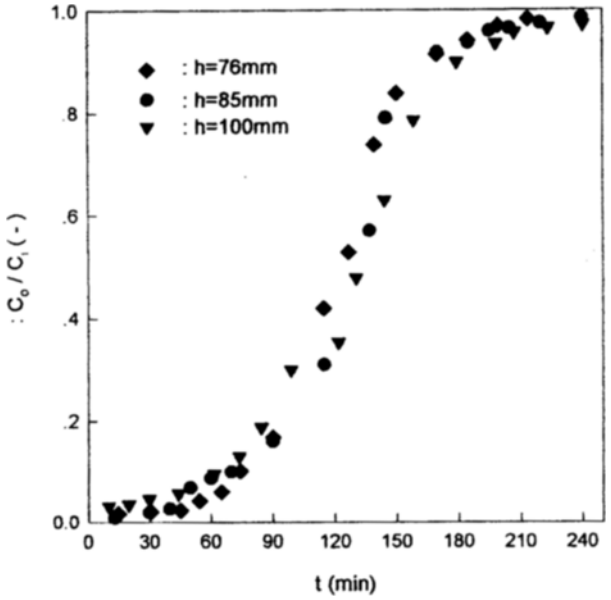

Fig. 7. Comparison of breakthrough data of Pb^{+2} ions in a semi-fluidized bed for different retaining grid heights.
U=5.33 U_{mf}, C_{Pb}=3 mN, resin weight=50 g

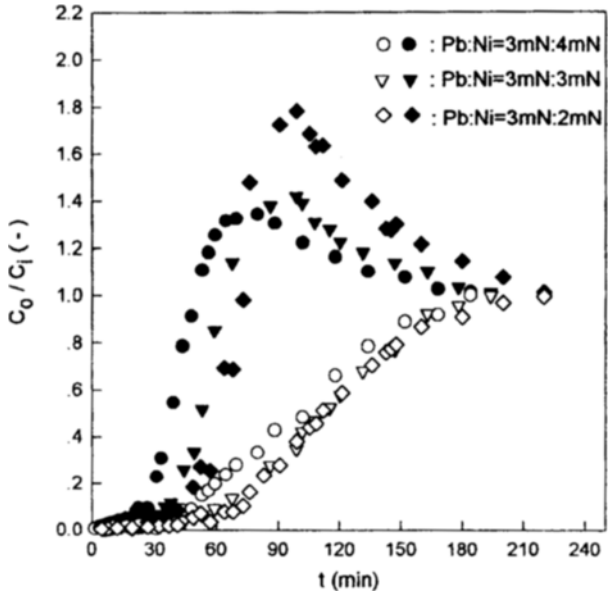

Fig. 8. Breakthrough data in a fixed bed for binary component solution.
U=5.33 U_{mf}, resin weight=50 g, ●▼◆: Ni^{+2}, ○▽◇: Pb^{+2}

those of the fixed and semi-fluidized beds initially but their values are completely reversed later. Furthermore, it should be noted that three breakthrough curves in Figs. 5 and 6 are similar regardless of the type of bed used. This unexpected result can be explained by the combined effect of axial dispersion and liquid-solid mass transfer. If one uses a fluidized bed, both the axial dispersion and mass transfer coefficients increase simultaneously. They have contrary effects on the stiffness of the breakthrough curve. The breakthrough time in general decreases with the fluid velocity or the inlet concentration.

As mentioned previously, the length of the fluidized bed section in the semi-fluidized bed can be changed by adjusting the position of retaining grid. Fig. 7 shows breakthrough curves for three different retaining grid heights under the same operating conditions. The retaining grid heights are 76, 85, and 100 mm, respectively. The breakthrough curve becomes more steep for lower retaining grid height, resulting in a longer breakthrough time even if the variation of the retaining grid height has only marginal effect on the breakthrough.

4. Breakthrough Curves of Binary Component Solution

Three typical binary breakthrough curves for Pb^{2+} and Ni^{2+} in a fixed bed were also obtained experimentally to study the mutual effect of two ions on each other as shown in Fig. 8. In these experiments, the concentration of Pb^{2+} was kept at 3 mN, while that of Ni^{2+} was changed from 2 mN to 4 mN. According to the difference in affinity to the resin, Ni^{2+} appears first at the exit and than the breakthrough curve of Ni^{2+} follows. In general, the species with the lowest affinity would appear first in multicomponent adsorption and ion-exchange column operation. As shown in Fig. 8, one can find the overshooting phenomenon in the breakthrough curve of the weaker species. This phenomenon could be explained by mutual interaction between two ions during their breakthroughs. At the initial stage, the strong species adsorbs or is ion-exchanged in the front section of the column, and the weak species flows down along the column and adsorbs in the rear section. After the front section is saturated with the strong species, it flows down and replaces with the weak species already attached in the rear section according to their affinities. This effect is the so-called "competitive adsorption or competitive ion-exchange". Such a mutual interaction in the column creates the overshooting phenomenon of the weak species in its breakthrough. In separating two species by a chromatographic column, when step concentration inputs are introduced, this competitive effect enhances the separation efficiency. The overshooting effect becomes larger as the concentration ratio between two species increases, depending on their equilibrium relation.

Fig. 9 shows three binary breakthrough curves from a semi-fluidized bed under the same experimental conditions used for the fixed bed as shown in Fig. 7. Even though the breakthrough curves are less stiff than those obtained from the fixed bed, there is no significant difference in their shape and breakthrough times. This implies that the use of a semi-fluidized bed instead of a fixed bed does not significantly reduce the separation efficiency. Considering the difference in pressure drops through the column as shown in Fig. 1, it may be concluded that a semi-fluidized operation has much greater benefit than a conventional fixed bed operation, at least for the removal of heavy metals by ion-exchange resins.

In Fig. 8 and 9, when binary solutions are passed through the bed, the breakthrough time to reach 10 % of the inlet concentration decreases, compared with single component systems. This result comes from the fact that the resin has a given amount of ion-exchange capacity. In any case, the breakthrough time for the fixed bed is longer than that for the semi-fluidized bed, since the effect of axial dispersion surpasses that of solid-liquid mass transfer.

Other breakthrough curves for the binary solutions are also

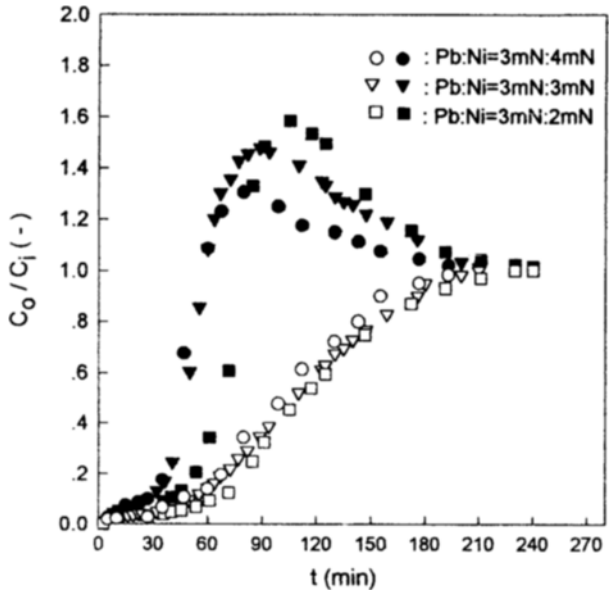

Fig. 9. Breakthrough data in a semi-fluidized bed for binary component solution.
h=85 mm, U=5.33 U_{mf}, resin weight=50 g, ●▼■: Ni^{+2}, ○▽□: Pb^{+2}

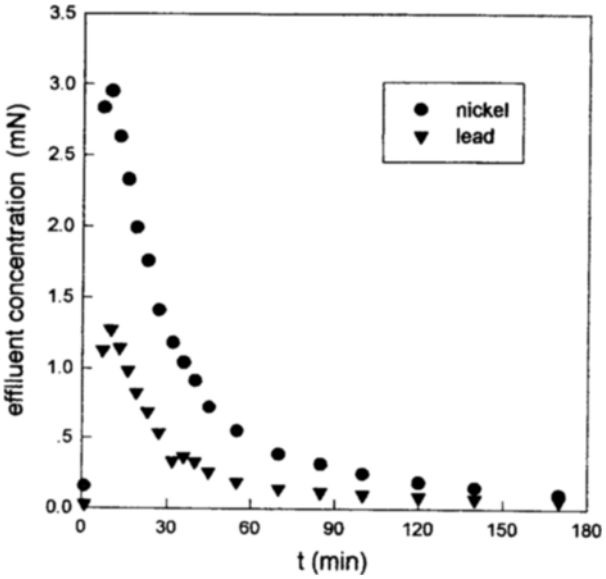

Fig. 10. Breakthrough data in a semi-fluidized bed for different lead concentration.
h=76 mm, U=6.68 U_{mf}, resin weight=50 g, ●▼◆: Ni^{+2}, ○▽◇: Pb^{+2}

measured and shown in Fig. 10. In this case, the concentration of Pb^{2+} was changed from 2 mN to 4 mN while that of Ni^{2+} was kept constant at 3 mN. All other experimental conditions were fixed. In Fig. 10, the breakthrough time increases as the total concentration decreases.

5. Separation and Recovery of Pb^{2+} and Ni^{2+} Ions

The final target of ion-exchange processes will be the separation of two metal ions for their reuse. Therefore some experiments were carried out to access the removal and separation efficiency. In these experiments, a binary solution was fed

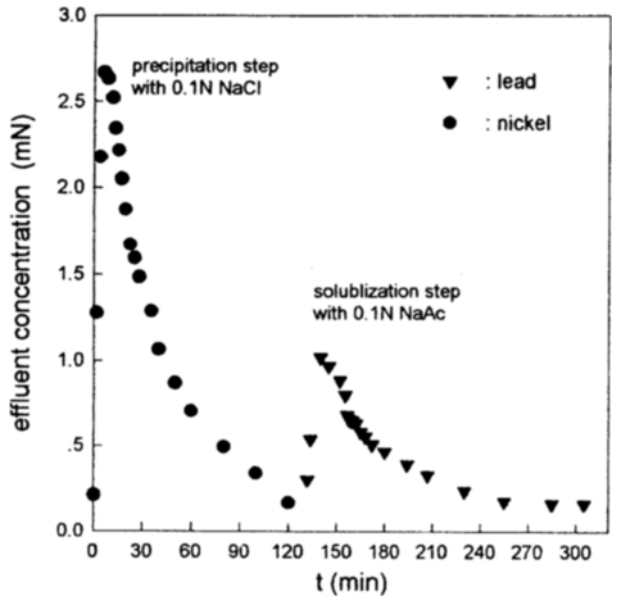

Fig. 11. Effluent concentration of Pb^{+2} and Ni^{+2} ions in the precipitation and solublization steps.
U=4.33 U_{mf}, C_{NaCl}=0.1 N, C_{NaAc}=0.1 N

to the fixed bed until the predetermined breakthrough time or the exit concentration of the weak ion reached 10 % of its inlet concentration. Under experimental conditions shown in Fig. 11, the breakthrough time was about 37 min. In Fig. 10, the total amount of Pb^{2+} and Ni^{2+} fed to the bed was 59.2 meq. The ion-exchange capacities of Pb^{2+} and Ni^{2+} ions were 56.97 meq and 53.59 meq, respectively. During the removal step, the development of green nickel front was experimentally observed.

After removal of Pb^{2+} and Ni^{2+} from the binary solution for a given time, 0.1 N NaCl solution was fed to the bed to precipitate Pb^{2+} as $PbCl_2$. Since most lead chloride precipitates remain inside the bed, the concentration of Pb^{2+} in the effluent

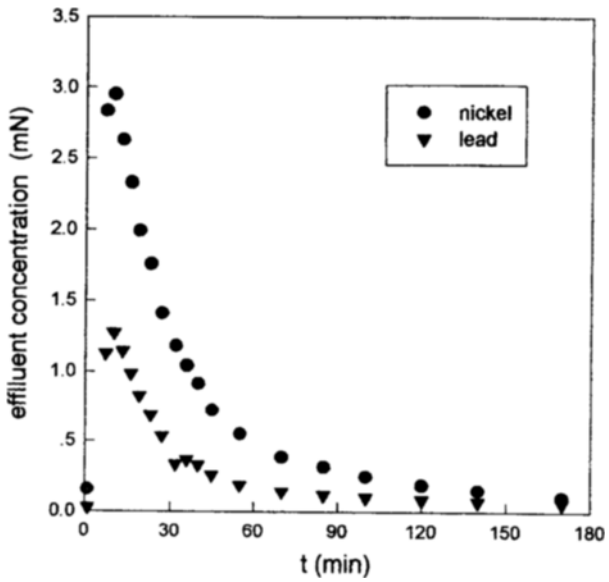

Fig. 12. Separation of Pb^{+2} and Ni^{+2} with sodium acetate solution without precipition step.
U=4.33 U_{mf}, C_{NaAc}=0.1 N

was measured to be below 0.008 mN while the concentration of Ni^{2+} was as high as 2.67 mN. In this step, the separation of Pb^{2+} and Ni^{2+} and the recovery of pure nickel were achieved at the same time, because Pb^{2+} stayed inside the bed as $PbCl_2$ precipitate and Ni^{2+} was eluted. The total amount of nickel collected was about 50.74 meq in the precipitation step. Therefore, the recovery yield of nickel was about 94 percent. When the elution of Ni^{2+} was completed, the feed stream was switched to 0.1 N NaAc (sodium acetate) solution to dissolve $PbCl_2$ precipitate in the bed. During elution of Pb^{2+} with the NaAc solution, the resin was regenerated. The total amount of pure Pb^{2+} recovered in the resolubilization step was about 25.5 meq. In this step, the maximum concentration of Pb^{2+} in the effluent was 1.02 mN. Fig. 11 shows the exit concentration profiles of Ni^{2+} and Pb^{2+} during the precipitation and resolubilization steps.

To check the effect of the precipitation step with 0.1 N NaCl, the elution curves of Pb^{2+} and Ni^{2+} were measured using a 0.1 N NaAc solution without the precipitation step. As shown in Fig. 12, the elution profiles of Pb^{2+} and Ni^{2+} were overlapped. This means that the complete separation of Pb^{2+} and Ni^{2+} cannot be done without the precipitation step. In this operation, the total amount of Pb^{2+} and Ni^{2+} recovered was about 27.6 meq.

CONCLUSIONS

Experiments were performed to investigate the removal and separation of Pb^{2+} and Ni^{2+} using a strong cation exchanger, Amberlite 200, in fixed and semi-fluidized beds. From ion-exchange equilibrium data, the resin has a higher selectivity for Pb^{2+} than Ni^{2+}, with the result that the breakthrough time of Pb^{2+} is longer than that of Ni^{2+} regardless of the type of bed. When binary solutions were fed into the bed, the breakthrough times of both ions decreased since the resin has a limited ion-exchange capacity. In binary systems, the breakthrough curve of the weak ion shows the overshoot, in which the exit concentration is over the inlet concentration. This phenomenon could be explained by the mutual interaction between two ions according to the difference in affinities. This overshoot phenomenon enhances the separation efficiency in most binary adsorption or ion-exchange processes.

According to breakthrough behavior of single and binary systems, the fixed bed operation gives more stiff breakthrough curves than the semi-fluidized operation. In other words, the breakthrough time of the fixed bed is longer than that of the semi-fluidized bed. However the type of bed does not affect the breakthrough curve significantly, as discussed in previous sections. Considering the difference in pressure drops, the semi-fluidized operation has a much better benefit than the fixed bed operation. One more special feature of the bed used in this study is to change the position of the retaining grid height, dividing the lower fluidized and upper fixed bed sections.

Furthermore, several experiments for separating two metal ions from their binary solutions were carried out using a cyclic operation, which consists of three major steps such as simultaneous isolation (or removal) of mixed ions, precipitation of lead ion as $PbCl_2$ by NaCl solution, and resolubilization of lead precipitate by sodium acetate solution. The final step stands for the regeneration of the resin. Since lead precipitate was retained in the bed during the precipitation step, almost pure nickel could be recovered. Finally, Pb was recovered from the bed by eluting the bed with 0.1 N sodium acetate solution. Without the precipitation step, Pb^{2+} and Ni^{2+} could not be separated.

ACKNOWLEDGEMENT

The authors with to acknowledge a grant-in a aid for research from the KOSEF (Grant No. 96-0502-01-3).

NOMENCLATURE

C_i : inlet concentration of reactant [mN]
C_o : effluent concentration of reactant [mN]
C_e : equilibrium lead (or nickel) ion concentration in the liquid phase [mN]
d_p : particle diameter [mm]
H : height of retaining grid in a semi-fluidized bed [mm]
h_0 : height of initial static bed [mm]
U : superstitial fluid velocity in axial direction [mm/s]
U_{mf} : minimum fluidization velocity [mm/s]
U_t : terminal velocity of the particle [mm/s]
x_i : equivalent fraction of ion i liquid phase [-]
y_i : equivalent fraction of ion i resin phase [-]
Q : ion-exchange capacity per unit mass of the resin [mg/g]

Greek Letter

α : separation factor [-]

REFERENCES

Anderson, R.E., "Ion Exchange Separations in Handbook of Separation Technique for Chemical Engineers," Section1. 12, McGraw-Hill, New York (1988).

Clifford, D., "Multicomponent Ion Exchange Calculation for Selected Ion Separation," *Ind. Eng. Chem. Fundam.*, **21**, 141 (1982).

Davidson, J.F. and Harrison, D., "Fluidization," Academic Press, London, p.36 (1977).

Fan, L.T., Yang, Y.C. and Wen, C.Y., "Mass Transfer in Semifluidized Beds for Solid-Particle System," *AIChE J.*, **6**, 482 (1960).

Fan, L.T., Yang, Y.C. and Wen, C.Y., "Semifluidization: Mass Transfer in Semifluidized Beds," *AIChE J.*, **5**, 407 (1959).

Hass, C.N. and Tare, V., "Application of Ion Exchangers to Recovery of Metals from Semiconductor Waste," *Reactive polymers*, **2**, 61 (1984).

Hwang, S.J. and Lu, W.J., "Ion Exchange in a Semifluidized Bed," *Ind. Eng. Chem. Res.*, **34**, 4, 1434 (1995).

Lee, K. and Hong, J., "Separation and Recovery of Lead by Cation Exchange Process Combined with Precipitation," *AIChE J.*, **41**, 12, 2653 (1995).

Maruyama, T., Hannah, S.A. and Cohen, J.H., "Metal Removal by Physical and Chemical Treatment Processes,"

Water Pollut. Control Fed. J., **47**, 962 (1975).
Patterson, J. W., "Wastewater Treatment Technology," Ann Arbor Science, Ann Arbor (1975).
Singh, A. N., Kesavan, s. and Gupta, P. S., "Rate of Mass Transfer in a Semifluidized Bed," *Int. J. Heat Mass Tr.*, **23**, 279 (1980).